Tunable and compact dispersion compensation of broadband THz quantum cascade laser frequency combs

Francesco Mezzapesa, Valentino Pistore, Katia Garrasi, Lianhe Li, A. Giles Davies, Edmund H. Linfield, Sukhdeep Dhillon, Miriam Vitiello

▶ **To cite this version:**

Francesco Mezzapesa, Valentino Pistore, Katia Garrasi, Lianhe Li, A. Giles Davies, et al.. Tunable and compact dispersion compensation of broadband THz quantum cascade laser frequency combs. Optics Express, 2019, 27 (15), pp.20231. 10.1364/OE.27.020231 . hal-02412975

HAL Id: hal-02412975
https://hal.science/hal-02412975v1

Submitted on 15 Oct 2024

HAL is a multi-disciplinary open access archive for the deposit and dissemination of scientific research documents, whether they are published or not. The documents may come from teaching and research institutions in France or abroad, or from public or private research centers.

L'archive ouverte pluridisciplinaire **HAL**, est destinée au dépôt et à la diffusion de documents scientifiques de niveau recherche, publiés ou non, émanant des établissements d'enseignement et de recherche français ou étrangers, des laboratoires publics ou privés.

Distributed under a Creative Commons Attribution 4.0 International License

Research Article | Vol. 27, No. 15 | 22 Jul 2019 | OPTICS EXPRESS 20231
Optics EXPRESS

Tunable and compact dispersion compensation of broadband THz quantum cascade laser frequency combs

FRANCESCO P. MEZZAPESA,[1] VALENTINO PISTORE,[2,4] KATIA GARRASI,[1,4] LIANHE LI,[3] A. GILES DAVIES,[3] EDMUND H. LINFIELD,[3] SUKHDEEP DHILLON,[2] AND MIRIAM S. VITIELLO[1,*]

[1]*NEST, CNR - Istituto Nanoscienze and Scuola Normale Superiore, Piazza San Silvestro 12, 56127 Pisa, Italy*
[2]*Laboratoire de Physique de l'Ecole Normale Supérieure, ENS, Université PSL, CNRS, Sorbonne Université, Université de Paris, Paris, France*
[3]*School of Electronic and Electrical Engineering, University of Leeds, Leeds LS2 9JT, UK*
[4]*Authors contributed equally to the work*
[*]*miriam.vitiello@sns.it*

Abstract: Miniaturized frequency combs (FCs) can be self-generated at terahertz (THz) frequencies through four-wave mixing in the cavity of a quantum cascade laser (QCL). To date, however, stable comb operation is only observed over a small operational current range in which the bias-depended chromatic dispersion is compensated. As most dispersion compensation techniques in the THz range are not tunable, this limits the spectral coverage of the comb and the emitted output power, restricting potential applications in, for example, metrology and ultrashort THz pulse generation. Here, we demonstrate an alternative architecture that provides a tunable, lithographically independent, control of the free-running coherence properties of THz QCL FCs. This is achieved by integrating an on-chip tightly coupled mirror with the QCL cavity, providing an external cavity and hence a tunable Gires Tournois interferometer (GTI). By finely adjusting the gap between the GTI and the back-facet of an ultra-broadband, high dynamic range QCL, we attain wide dispersion compensation regions, where stable and narrow (~3 kHz linewidth) single beatnotes extend over an operation range that is significantly larger than that of dispersion-dominated bare laser cavity counterparts. Significant reduction of the phase noise is registered over the whole QCL spectral bandwidth (1.35 THz). This agile accommodation of a tunable dispersion compensator will help enable uptake of QCL-combs for metrological, spectroscopic and quantum technology−oriented applications.

Published by The Optical Society under the terms of the Creative Commons Attribution 4.0 License. Further distribution of this work must maintain attribution to the author(s) and the published article's title, journal citation, and DOI.

1. Introduction

Terahertz (THz) frequency quantum cascade lasers (QCLs) [1,2] are compact semiconductor devices which are capable of delivering ultrabroadband spectral bandwidths [3–5], Watt-level output powers [6], and quantum-limited linewidths [7], making these sources particularly advantageous for high-resolution broadband THz spectroscopy [8], high precision frequency metrology [9], and for still unexplored applications in attosecond science [10].

Broadband frequency coverage in THz QCLs can be routinely achieved by designing heterogeneous quantum cascade active regions [11,12], in which flat-top gain profiles are achieved over the THz bandwidth, providing an intrinsically low chromatic dispersion. Consequently, phase-locking of lasing modes occurs through intracavity nonlinear four wave mixing (FWM), which arises from the inherently high third-order susceptibility [13,14]. This

#354776 https://doi.org/10.1364/OE.27.020231
Journal © 2019 Received 6 Dec 2018; revised 28 May 2019; accepted 4 Jun 2019; published 9 Jul 2019

Optics EXPRESS

enables the generation of frequency combs (FCs), [15,3] comprising uniformly spaced spectral lines, without any additional mode-locking mechanism [15,13].

Although group delay dispersion (GDD) can be low in a THz QCL, stable comb operation is typically restricted to a relatively small fraction of the QCL dynamic range, [15,3,5,12] owing to the strong electric field-dependence of the GDD associated with the intersubband transitions, inherent in heterogeneous QCL designs. This limits the spectral range of the QCL comb. In order to allow FC operation over the entire laser dynamic range and spectral bandwidth, accurate control of the dispersion between different subsets of longitudinal modes needs to be achieved.

Recently, an effective increase of the dynamic range of operation of a QCL comb has been demonstrated in the mid-IR by building an external cavity set-up for a tunable Gire-Tournois interferometer (GTI) approach [16].

However, engineering and compensating the cavity dispersion at THz frequencies is more demanding, due to the fact that semiconductor materials are much more dispersive at THz frequencies, the heterogeneous active regions exploit large gain bandwidths and lasers operate only at cryogenic temperatures. Sophisticated schemes to fully [17] or partially [15,18] compensate the GDD dispersion have been therefore recently proposed and implemented [15,17,18]. For example, a double chirped mirror-like architecture was incorporated into a tapered ridge waveguide to induce FC operation in a THz QCL with an homogeneous gain medium [15]. Its corrugation length and tapering period were designed to optimize the cavity GDD and achieve low dispersion over the frequency range of interest, although comb operation could cover only 28% of the full laser dynamic range. In an alternative approach, stable comb operation was demonstrated over the entire laser range by modifying a Fabry-Perot (FP) QCL into a two-section cavity, in which a second biased section was separated from the main laser cavity by ~2 μm [17]. The narrow air gap allowed the two sections to be optically coupled whilst simultaneously enabling electrical isolation. The bias-dependent dispersion associated with the intersubband transitions in the main cavity was then compensated by electrically tuning the extra section. This led to FCs spanning 600 GHz, centred at 3.5 THz. However, only a few, unevenly spaced, optically active modes were obtained, and these had dissimilar and irregular intensities [17]. Following a similar approach, a GTI was monolithically integrated into a THz QCL cavity to introduce chromatic dispersion opposite to that of the gain medium [18]. Effective GDD compensation was, however, only achieved over a specific frequency range, defined by the GTI length, owing to oscillation in the group delay dispersion, as the phase of the reflected light, and therefore the GDD, changed periodically with the optical frequency as a result of resonances. Nevertheless, ultra-short THz pulses were demonstrated with this approach, at the expense of the stringent, geometrical constraint of a precise, lithographically pre-defined GTI length.

2. Experimental set-up and simulations

In this paper, we demonstrate a tunable scheme for compensating the GDD over the majority of the laser operational range and spectral bandwidth, while achieving evenly spaced optical modes with similar intensities. We engineer a mechanically tunable GTI by positioning a moving gold retro-reflector in close proximity to the back facet of a THz QCL (Fig. 1(a)) Our rationale is to exploit the QCL sensitivity to back reflected radiation [19] in a Gires Tournois etalon [20] -like configuration. In our case, a high reflectivity external mirror ($r^2 \approx 1$ over the QCL bandwidth, where r is the field reflectivity) is positioned parallel to the QCL facet to tune the optical feedback experienced by the QCL and hence optimise frequency comb synthesis. The phase of the reflected light tunes the total cavity dispersion (Fig. 1(a)).

Optics EXPRESS

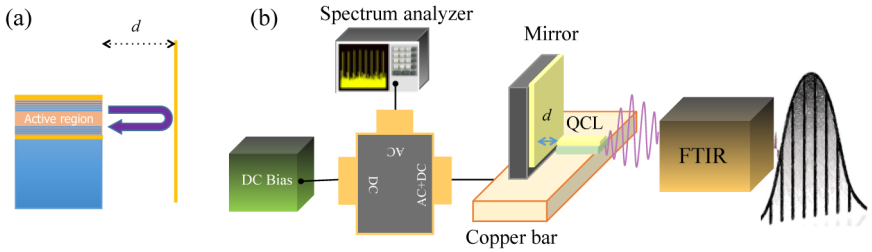

Fig. 1. Chip-scale Gires-Tournois interferometer (GTI). (a) Principle of the external GTI. A part of the light emitted from the back facet is reflected back into the waveguide mode. (b) Device schematic: a THz QCL is integrated with an external metal etalon (gold mirror), which defines a Gires-Tournois interferometer, of tunable length, providing chromatic dispersion for the THz QCL comb. The gold mirror positioned on a piezoelectric actuator was tightly coupled to the back-facet of a heterogeneous THz QCL, without exploiting any focusing optics, and integrated onto a cold-finger cryostat.

A GTI usually consists of a small resonator with dielectric coatings, with a length that is typically the same order as the wavelength in the laser cavity, or an integer multiple of half wavelengths. In the most ideal geometry, the GTI operates in reflection with a front mirror of low reflectivity and a back mirror, which is perfectly reflective. Under these conditions, one can ensure that the reflectivity is kept constant over the whole frequency range of the laser, with the phase varying with the external cavity length. This means that GDD can be both positive and negative over the entire laser operational range. Our experimental arrangement in depicted schematically in Fig. 1(b). A gold mirror positioned on a piezoelectric actuator was tightly coupled to the back-facet of a heterogeneous THz QCL, without exploiting any focusing optics, and integrated onto a cold-finger cryostat.

The THz QCL used in our work comprised a 17-μm-thick GaAs/AlGaAs heterostructure with three active region modules, each exploiting a resonant phonon depopulation scheme but with frequency-detuned gain bandwidths centred at 2.5 THz, 3 THz and 3.5 THz. Laser bars were fabricated in a Au-Au metal–metal waveguide geometry, [11,2] and lossy side absorbers were lithographically implemented along the waveguide edges to inhibit lasing of the higher order lateral modes [5]. The final device shows a very broad operational dynamic range, $J_{dr} = J_{max}/J_{th} = 3.2$, where J_{max} is the maximum working current density and J_{th} the threshold current density.

In order to reduce the residual GDD of the QCL, and facilitate phase locking between lasing modes, a chromatic dispersion opposite to that arising in the QCL cavity has to be intentionally introduced within the frequency range of interest. To achieve this, we finely adjusted the external cavity length of the GTI, by micro-positioning the mirror with respect to the QCL back facet. By tuning the external cavity length in this way, we induced compensation of both material and gain dispersion (the waveguide dispersion is assumed to be negligible).

By exploiting both the positive and the negative GDD regimes of the GTI, we compensate for positive and negative gain GDD in the laser cavity. Numerical simulations of the dispersion compensation were performed (Figs. 2(a) and 2(b)) using a finite element method (Comsol Multiphysics).

Optics EXPRESS

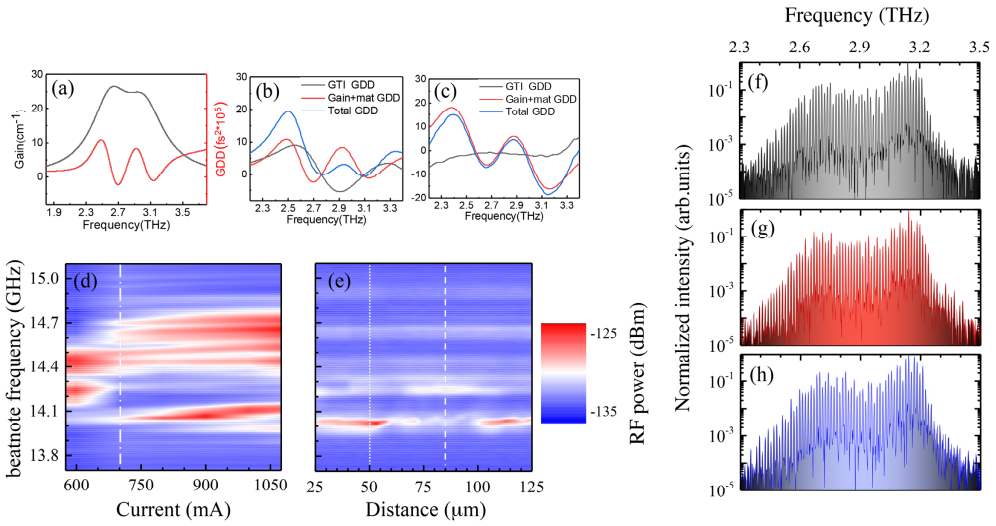

Fig. 2. Tunable dispersion compensation. **(a-b)** The gain of the QCL (black) is shown as a function of frequency in (a), together with the corresponding GDD (red). In (b), the individual simulated GTI GDD, the material and gain GDD, and the total GDD are shown for a specific GTI length of 55μm, corresponding to the 'on-resonance' position. **(c)** Individual simulated GTI GDD, the material and gain GDD, and the total GDD for a specific GTI length of 80μm, corresponding to the 'off-resonance' position. **(d)** Inter-mode beat-note map as a function of drive current obtained at 15 K from a 2.9-mm-long, 85-μm-wide laser bar operating in continuous wave (CW). The beat-note signal is extracted from the bias line using a bias-tee, and is recorded with an RF spectrum analyzer (Rohde & Schwarz FSW; resolution bandwidth (RBW): 500 Hz, video bandwidth (VBW): 500 Hz, sweep time (SWT): 20 ms, RMS acquisition mode). **(e)** Evolution of the electrical beat-note spectra of a THz QCL coupled to a Gires-Tournois etalon as a function of the position of the external mirror, for a fixed driving current of 700 mA (dash dot line in panel (c)). The dotted (dashed) vertical lines mark a prototypical GTI 'on resonance' ('off resonance') length. **(f-h)** FTIR spectra collected in rapid scan mode, under vacuum with a 0.075 cm^{-1} resolution at 15 K, whilst driving the QCL in continuous-wave at 700 mA and keeping the external mirror at a distance of (f) d = 55 μm from the QCL back facet: ('on resonance' GTI), (g) d = 80 μm ('off resonance' GTI), or (h), without the external mirror (bare THz QCL laser facet).

The simulated structure includes the end of the QCL waveguide and a gold mirror at a separation 'd' from the laser facet, surrounded at a distance of a few λ by vacuum and absorbing boundary conditions. THz radiation is injected into the QCL waveguide (from the end opposite to the GTI) and is reflected back into the QCL waveguide by the GTI. This allows one to obtain the amplitude and phase of the S_{11} scattering parameter. Finally, the dispersion provided by the structure is computed from the second derivative of the phase.

The final dispersion profile takes into account the contributions from the material and gain of the QCL, as well as that of the GTI. The approach used in [20] was employed to compute the first two terms. A Drude-Lorentz model for the frequency dependent refractive index of the material was considered, and its deviation due to the QCL's gain, obtained from the Kramers-Kronig equations, was added. The waveguide dispersion contribution is negligible with respect to the other terms, and was therefore neglected.

Figure 2(a) shows, in black, the assumed gain profile of the laser, made up of two Lorentzian functions centered at 2.6 and 3.1 THz according to the emission spectra of the QCL (the laser section that was designed to work at 3.5 THz does not show laser action, and so has been omitted), with the corresponding GDD shown in red. Figure 2(b) then shows the material and gain contribution to the GDD (red), the GDD provided by the GTI with the gold mirror 55 μm away from the QCL facet (black), and the corresponding total GDD (blue). At

Optics EXPRESS

this mirror separation, the total GDD is reduced over a large spectral range (~2.7 – 3.1 THz). The effect is periodic owing to the Fabry-Perot resonances of the cavity, and so outside this region, the GTI does not lead to a reduction in the GDD associated with the gain. Vice-versa when the gold mirror is positioned at 80 μm from the QCL facet the total GDD does not show any remarkable variation (Fig. 2(c)).

3. Results and discussion

To characterize the mode coherence of the free running THz QCL, we performed beat-note spectroscopy measurements at different points on the current-voltage characteristic. (Further details on the continuous wave electrical characteristics of the investigated QCL can be found in Refs. 5 and 11.) Beat-notes were extracted using a bias-tee connected to a commercial Rohde & Schwarz spectrum analyser in its root mean square (RMS) acquisition mode. A visible dispersion-dominated regime, at $J/J_{th} \geq 1.4$ (600mA), is seen in Fig. 2(d) for the bare THz QCL laser cavity driven in continuous-wave (CW) by a low-noise power supply (Wavelength Electronics) at a fixed heat-sink temperature of 15 K. The broad range of beat-notes indicates that the group velocity dispersion is large enough to prevent FWM from locking the lasing modes in frequency and phase, simultaneously. Furthermore, the heterogeneous nature of the active region entangles the dispersion dynamics at large biases, meaning that the THz QCL behaves like a conventional multi-mode laser [5].

Figure 2(e) shows, at a fixed bias point (V = 8.9V; I = 700mA), the evolution of the electrical beatnote of the THz QCL coupled to the gold mirror as a function of mirror position. A narrow and strong beatnote at the laser repetition rate ($f_{rep} = c/2nL$, where L is the cavity length and n the effective refractive index of the material) is unveiled for periodic positions of the external mirror, i.e. by tuning the air gap between the Au mirror and the laser facet, which define an external cavity (our GTI) of tunable length d. At periodic mirror positions, effective dispersion compensation is achieved, which correspond to the 'on-resonance' GTI regime, i.e. to the condition in which the GTI resonant frequency matches the central emission frequency of the heterogeneous QCL gain bandwidth; GDD compensation thus occurs periodically.

The emission spectra collected under vacuum using a commercial Fourier-transform infrared (FTIR) spectrometer (Bruker v80) operating in rapid scan mode (Fig. 2(f)–2(h)) feature a large number (>100) of modes lasing simultaneously over a spectral bandwidth of 1.3 THz (from 75 cm^{-1} to 118.5 cm^{-1}). The comparison between the prototypical CW optical spectra measured on the bare laser cavity (Fig. 2(h)) at a current of 700 mA, and those acquired from the mirror-coupled QCL at distances corresponding to a GTI 'on resonance' (Fig. 2(f)) and 'off-resonance' (Fig. 2(g)), does not show significant changes in the mode spacing/shaping, ascribable to the GTI dispersion compensator. Although each mode experiences an effective feedback which is periodically modulated by varying the external cavity length of the GTI, and even though small feedback differences may affect the competition mechanisms amongst the lasing modes [18], the resolution of the FTIR spectrometer (2.25 GHz) is not sufficient to identify visible spectral changes in the broadband laser spectrum.

Beat-note maps are presented in Figs. 3(a)–3(c), where the electrical beat-note is plotted as a function of QCL bias current. In contrast to the FTIR spectra, these maps show clearly the advantages of utilising an externally-coupled GTI approach. The 'on-resonance GTI' (Fig. 3(a)) leads to a significant enlargement of the intracavity dynamic range for the FC, compared with results from a bare THz QCL laser cavity (Fig. 3(c)). Below 580 mA, the individual narrow beat-note observed just above threshold (~430 mA, J_{th} ~170 A/cm^2) is seen to be preserved over a continuous 150 mA current range (430-580 mA, Fig. 3(a)) for the dispersion-compensated QCL comb (GTI 'on resonance'), which is almost 35% wider than that recorded in the bare THz QCL laser cavity (430-536 mA, Fig. 3(c) [5]. Correspondingly, in the 'on resonance' regime, the beatnote frequency shifts to values in the range 14.8-14.9

Optics EXPRESS

GHz. In contrast, for the 'off resonance' GTI (Fig. 3(b)) there is a reduction of the single beat-note current range to 92 mA (430-522 mA).

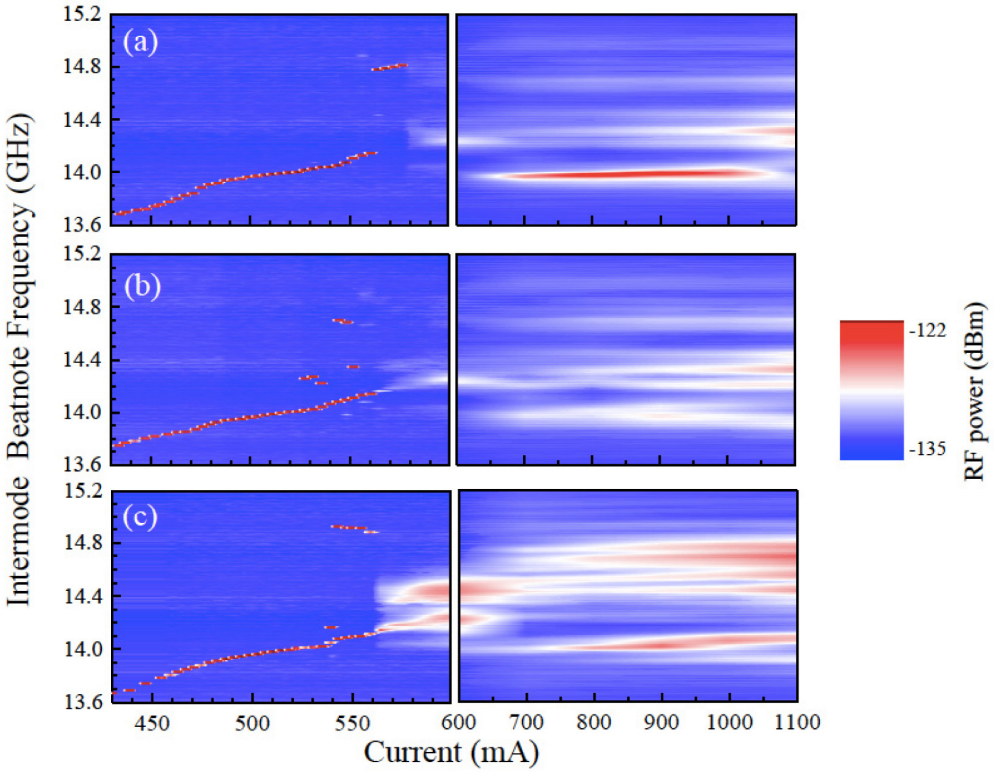

Fig. 3. Intermode beat-note maps. **(a-b)** Electrical beat-note map as a function of QCL bias current for a 2.9 mm long, 85 µm wide laser bar with a GTI of tunable length, operating (a) 'on-resonance', d = 55µm, and (b) 'off-resonance', d = 80µm (b). **(c)** Evolution of the beat-note signal for the bare QCL laser cavity. All measurements were performed CW at 15 K. The beat-note signal is extracted from the bias line with a bias-tee and is recorded with an RF spectrum analyzer (Rohde & Schwarz FSW; resolution bandwidth (RBW): 500 Hz, video bandwidth (VBW): 500 Hz, sweep time (SWT): 20 ms, RMS acquisition mode).

As the current is progressively increased through these dynamic ranges, the beat-note red-shifts with QCL drive current for the 'off-resonance' and 'on-resonance' GTI, as well as for the case of the bare laser cavity. This is a result of the chromatic dispersion in the gain spectrum. However, the beat-notes for the bare laser cavity (Fig. 3(c)) exhibit a multi-mode regime between 540 and 543mA, ascribable to higher order lateral modes, which is followed by a dual-comb regime between 544 and 560mA; this reflects the dual-comb nature of the heterogeneous active region core. Between 560 and 580 mA, a wide beat-note is then seen, which broadens progressively with increasing bias. In contrast, neither the multi- nor the dual-beat-note regimes occur in the 'on-resonance' GTI, by progressively increasing the bias current up to 580 mA. This is likely to be a result of the dispersion compensation mechanism suppressing higher order lateral modes from reaching threshold, and simultaneously locking the phase of the two families of modes centred at ~2.7 THz and ~3.1 THz, which result from the heterogeneous gain media [13]. Conversely, examining the 'off-resonance GTI' (Fig. 3(b)), a multi-mode regime is seen to extend over a wider dynamic range (522-560mA), with a lack of any clear beat-note above 560 mA.

The results above 580 mA are, however, more remarkable. For the bare laser cavity, a region of high phase noise is seen (Fig. 3(c)), caused by loss of the FWM self phase-locking

Optics EXPRESS

mechanism owing to high GDD. In contrast, for the 'on-resonance' GTI-coupled QCL (Fig. 3(a)), the high phase noise is greatly suppressed, enabling access to a new operating regime where a single beat-note persists over an extremely wide dynamic range (650-980 mA), remains superimposed to a broader bandwidth and slightly tunes by increasing the current (Fig. 3(a)). For comparison, when the GTI operates 'off-resonance' (Fig. 3(b)) no beat-notes are seen above 560mA, meaning that the separate modes lose their phase coherence.

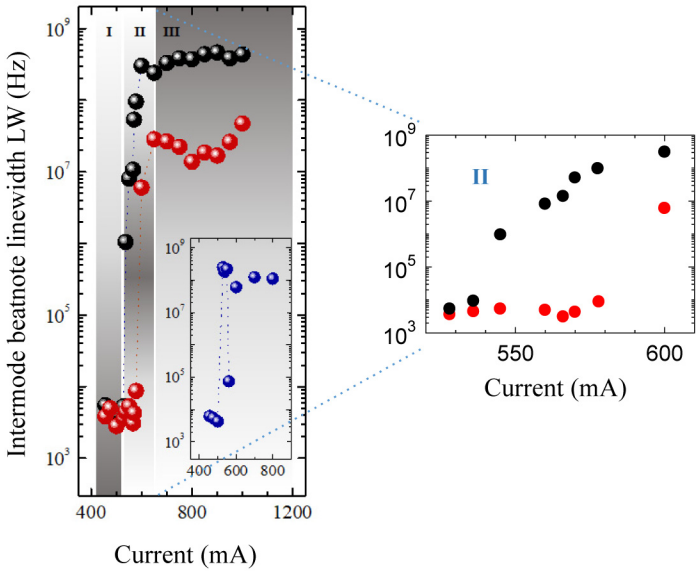

Fig. 4. Analysis of beat-note linewidth. **a)** Inter-mode beat-note linewidth plotted as a function of the driving current for the 'on-resonance' GTI integrated THz QCL (red dots), with the bare THz QCL laser cavity (black dots) acting as a reference. Inset: Corresponding inter-mode beat-note linewidth for the 'off-resonance' GTI integrated THz QCL. All measurements were performed in CW at 15 K. The beat-note signal is extracted from the bias line using a bias-tee connected to a RF optical spectrum analyzer (OSA) in RMS acquisition mode. Three distinct regions are marked on the graph: I) the narrow single beat-note regime (OSA setting: RWB: 10 kHz, VBW: 100 kHz, SWT: 500 ms); II) the 'on resonance' GTI-coupled THz QCL preserves the narrow single beat-note regime as a distinct comb regime around 14.9 GHz (OSA setting: RWB: 10 kHz, VBW: 100 kHz, SWT: 500 ms); III) the broad beat-note regime for the 'on resonance' GTI-coupled THz QCL frequency comb (OSA setting: RWB: 500 Hz, VBW: 500 Hz, SWT: 20 ms).

Figure 4 summarizes this complex beatnote evolution. Three distinctive regimes can be identified. In region I, the beat-note linewidth remains practically unperturbed; it is jitter-limited, as the QCL is not stabilized in frequency. Any reduction in the QCL linewidths (~3 kHz) with the 'on-resonance' GTI, compared with the case of the bare laser cavity (~5 kHz), are probably a result of the GTI integration improving the phase-locking of the lasing modes at certain biases. For comparison, no changes in the beat-note linewidth compared with the case of the bare QCL laser cavity are observed when the GTI operates 'off-resonance' (inset Fig. 4(a)).

Region II clearly highlights the advantages provided by using an 'on-resonance' GTI. For the case of a bare THz QCL cavity, increasing the drive current above 520 mA leads to a progressive broadening of the linewidth, which is a signature that the GVD becoming large enough to prevent the FWM from locking lasing modes in frequency and phase simultaneously. Specifically, the linewidth suddenly increases to > 100 MHz. Conversely, for the 'on-resonance' GTI, the linewidth first decreases to 2 kHz, and then remains practically constant up to 576 mA. It then progressively broadens first to 10 kHz (at 580 mA) and then 10 MHz (at 750 mA). This is reflected in the comparison between the RF beat-notes

Optics EXPRESS

measured at 576 mA in the 'on-resonance' and 'off-resonance' GTI-coupled QCL (Figs. 5(e) and 5(f)), and in the corresponding FTIR spectra (Figs. 5(a) and 5(b)), which unveil a rich and evenly spaced number of modes, having dissimilar intensities, spanning a 1 THz bandwidth (2.3 – 3.3 THz) in the 'on-resonance' GTI-coupled QCL (Fig. 5(a)).

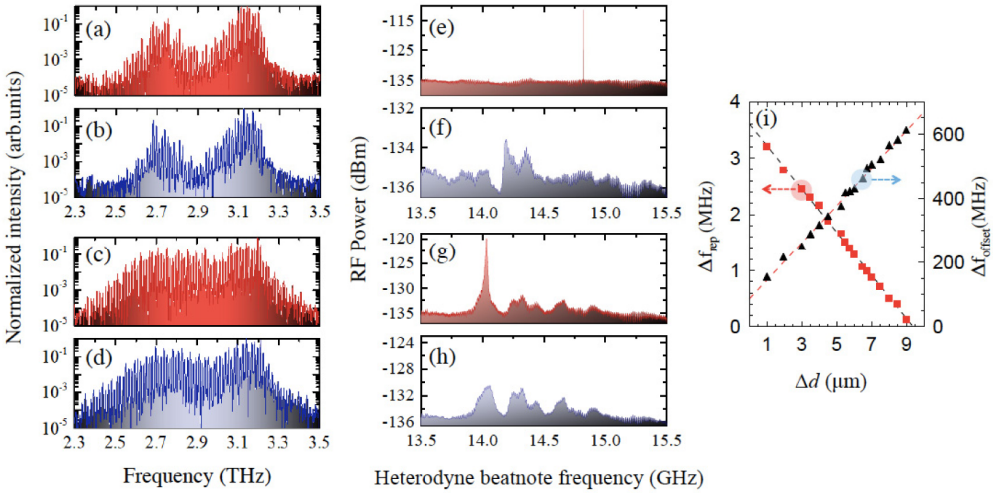

Fig. 5. Spectra, beat-notes and tuning of the repetition rate and carrier offset frequency. **(a-d)** FTIR spectra collected under vacuum in rapid scan mode, with a 0.075 cm^{-1} resolution, whilst driving the QCL at 15 K CW at (a-b) 576 mA and (c-d) 800 mA, for the (a,c) 'on-resonance' GTI-coupled THz QCL and (b,d) the 'off-resonance' GTI-coupled THz QCL. **(e-h)** Corresponding RF signals measured for (e,g) the 'on-resonance' (d = 55μm), and (f,h) 'off-resonance' (d = 80μm) GTI-coupled THz QCL at (e,f) 576 mA, and (g,h) 800 mA. **(i)** Tuning of f_{rep} (left vertical axis, squares) and f_{offset} (right vertical axis, triangles) as function of the relative distance between two mirror positions Δd, measured while driving the QCL at a current of 570 mA. The dashed lines are linear fits to the data.

In Region III, a wider individual beat-note is visible in the 'on-resonance' GTI-coupled QCL, which remains approximately constant (at ~10 MHz) over the whole operational QCL range (Fig. 5(g)). Although wider than in region I, this beat-note could still be locked to a microwave reference to enable reduction in the beat-note width [21]. Conversely, the bare laser cavity and the 'off-resonance' GTI-coupled QCL (inset Fig. 4) does not show a specific individual linewidth, but a broad band with an average 300 MHz linewidth (Fig. 5(h)). The corresponding CW FTIR spectra at 800 mA do not unveil clear distinctive changes in the mode spacing/intensity (Fig. 5(c) and 5(d)). The wider beatnote suggests that at high currents the dispersion is not entirely compensated, owing to two effects. As can be seen in Fig. 2(a) and 2(b), although the dispersion is compensated in the central part of the QCL spectrum, the total dispersion is greater at the extremities. As the current is increased, the spectral bandwidth increases and therefore the laser modes and these frequencies are not entirely compensated. Secondly, the gain itself has a dependence on bias [22], with the GVD determined by the intersubband gain in the active region that can vary with applied field, although this is lower when compared to the dispersion at the extremities of the spectrum.

Since the phase changes, induced by the GTI, depend on the tunable mirror position, the frequency of the cavity modes can be tuned by changing the mirror distance. We therefore extrapolated the tuning of the repetition rate f_{rep} and of the carrier offset frequency f_{offset} as a function of the relative distance Δd between individual mirror positions [16]. While $\Delta f_{rep}/\Delta d$ can directly extracted by measuring the corresponding beatnotes on the spectrum analyzer, $\Delta f_{offset}/\Delta$d has been extracted by comparing the interferograms at the individual mirror positions; indeed the periods of the interferogram fringes depends on both f_{rep} and f_{offset}, meaning that the intreferogram changes its fringes distances when f_{rep} and f_{offset} vary. To

Optics EXPRESS

extract the difference in the carrier offset frequency Δf_{offset}, we therefore calculated the distance between the zero-crossings of the fringes. The tuning of f_{rep} and f_{offset} as a function of the displacement of the on-chip mirror in a range of different position spanning 10μm is shown in Fig. 5(i). f_{rep} and f_{offset} show opposite tuning behaviors. The first, as expected, decreases linearly as the mirror distance is increased, with a slope $\Delta f_{rep}/\Delta d \approx 380$ kHz/μm. Vice-versa, the offset frequency tunes with a much larger slope $\Delta f_{offset}/\Delta d \approx 60$ MHz/μm. This implies that the external GTI provides a tool for independent tuning of f_{rep} and f_{offset}, enabling to possible full frequency stabilization of the comb [23].

4. Conclusions

In conclusion, we demonstrate that the free-running coherence properties of broadband THz QCLs, with a heterogeneous active region core, can be *modified* effectively through the chip-scale integration of a GTI micro-cavity, comprising a gold mirror and the QCL back facet. This enables adjustable compensation of chromatic dispersion. Continuous tuning of the feedback re-injected into the QCL waveguide then enables gain competition amongst the lasing modes to be modulated, and provides a unique capability for post-fabrication control of GDD. Further improvements in GDD compensation can be realized by optimizing the feedback from the gold mirror (e.g. by using angled or curved mirrors), where electromagnetic simulations have shown that this would permit the total GDD to be further tuned by engineering the phase of the reflected light. The agile accommodation of a tunable on-chip micro-cavity thus provides a route to develop zero inherent dispersion in THz QCL FCs, offering a breadth of prospects for applications including high-resolution molecular spectroscopy, fundamental time metrology, optical coherent tomography and quantum technology.

Funding

Horizon 2020 Framework Program 665158 (ULTRAQCL); H2020 European Research Council project 681379 (SPRINT); UK's Engineering and Physical Sciences Research Council (EP/P021859/1).

Acknowledgments

EHL is grateful for support from the Royal Society and Wolfson Foundation.

Disclosures

The authors declare that there are no conflicts of interest related to this article.

References

1. R. Köhler, A. Tredicucci, F. Beltram, H. E. Beere, E. H. Linfield, A. G. Davies, D. A. Ritchie, R. C. Iotti, and F. Rossi, "Terahertz semiconductor-heterostructure laser," Nature **417**(6885), 156–159 (2002).
2. M. S. Vitiello, G. Scalari, B. Williams, and P. De Natale, "Quantum cascade lasers: 20 years of challenges," Opt. Express **23**(4), 5167–5182 (2015).
3. M. Rösch, G. Scalari, M. Beck, and J. Faist, "Octave-spanning semiconductor laser," Nat. Photonics **9**(1), 42–47 (2015).
4. D. Turčínková, G. Scalari, F. Castellano, M. I. Amanti, M. Beck, and J. Faist, "Ultrabroadband heterogeneous quantum cascade laser emitting from 2.2 to 3.2 THz," Appl. Phys. Lett. **99**(19), 191104 (2011).
5. K. Garrasi, F. P. Mezzapesa, L. Salemi, L. Li, L. Consolino, S. Bartalini, P. De Natale, A. G. Davies, E. H. Linfield, and M. S. Vitiello, "High dynamic range, heterogeneous, terahertz quantum cascade lasers featuring thermallytunable frequency comb operation over a broad current range," ACS Photonics **6**(1), 73–78 (2019).
6. L. Li, L. Chen, J. Zhu, J. Freeman, P. Dean, A. Valvanis, A. G. Davies, and E. H. Linfield, "Terahertz quantum cascade lasers with >1 W output powers," Electron. Lett. **50**(4), 309–311 (2014).
7. M. S. Vitiello, L. Consolino, S. Bartalini, A. Taschin, A. Tredicucci, M. Inguscio, and P. De Natale, "Quantum-limited frequency fluctuations in a terahertz laser," Nat. Photonics **6**(8), 525–528 (2012).
8. S. Bartalini, L. Consolino, P. Cancio, P. De Natale, P. Bartolini, A. Taschin, M. De Pas, H. Beere, D. A. Ritchie, M. S. Vitiello, and R. Torre, "Frequency-comb-assisted Terahertz quantum cascade laser spectroscopy," Phys. Rev. X **4**(2), 021006 (2014).

Optics EXPRESS

9. S. Bartalini, M. S. Vitiello, and P. De Natale, "Quantum cascade lasers: a versatile source for precise measurements in the mid/far-infrared range," Meas. Sci. Technol. **25**(1), 012001 (2014).
10. T. W. Hänsch and N. Picqué, "Laser Spectroscopy and Frequency Comb," J. Phys. Conf. Ser. **467**, 012001 (2013).
11. L. H. Li, K. Garrasi, I. Kundu, Y. J. Han, M. Salih, M. S. Vitiello, A. G. Davis, and E. H. Linfield, "Broadband heterogeneous terahertz frequency quantum cascade laser," Electron. Lett. **54**(21), 1229–1231 (2018).
12. M. Rösch, M. Beck, S. Martin, D. Bachmann, K. Unterrainer, J. Faist, and G. Scalari, "Heterogeneous terahertz quantum cascade lasers exceeding 1.9 THz spectral bandwidth and featuring dual comb operation," Nanophotonics **7**(1), 237–242 (2018).
13. J. B. Khurgin, Y. Dikmelik, A. Hugi, and J. Faist, "Coherent frequency combs produced by self frequency modulation in quantum cascade lasers," Appl. Phys. Lett. **104**(8), 081118 (2014).
14. A. Hugi, G. Villares, S. Blaser, H. C. Liu, and J. Faist, "Mid-infrared frequency comb based on a quantum cascade laser," Nature **492**(7428), 229–233 (2012).
15. D. Burghoff, T.-Y. Kao, N. Han, C. W. I. Chan, X. Cai, Y. Yang, D. J. Hayton, J.-R. Gao, J. L. Reno, and Q. Hu, "Terahertz laser frequency combs," Nat. Photonics **8**(6), 462–467 (2014).
16. J. Hillbrand, P. Jouy, M. Beck, and J. Faist, "Tunable dispersion compensation of quantum cascade laser frequency combs," Opt. Lett. **43**(8), 1746–1749 (2018).
17. Y. Yang, D. Burghoff, J. Reno, and Q. Hu, "Achieving comb formation over the entire lasing range of quantum cascade lasers," Opt. Lett. **42**(19), 3888–3891 (2017).
18. F. Wang, H. Nong, T. Fobbe, V. Pistore, S. Houver, S. Markmann, N. Jukam, M. Amanti, C. Sirtori, S. Moumdji, R. Colombelli, L. Li, E. Linfield, G. Davies, J. Mangeney, J. Tignon, and S. Dhillon, "Short Terahertz pulse generation from a dispersion compensated modelocked semiconductor laser," Laser Photonics Rev. **11**(4), 1700013 (2017).
19. F. P. Mezzapesa, L. L. Columbo, M. Brambilla, M. Dabbicco, S. Borri, M. S. Vitiello, H. E. Beere, D. A. Ritchie, and G. Scamarcio, "Intrinsic stability of quantum cascade lasers against optical feedback," Opt. Express **21**(11), 13748–13757 (2013).
20. F. Gires and P. Tournois, "Interferometre utilisable pour la compression d'impulsions lumineuses modulees en frequence," C R Acad Sci Paris **258**, 6112 (1964).
21. P. Gellie, S. Barbieri, J. F. Lampin, P. Filloux, C. Manquest, C. Sirtori, I. Sagnes, S. P. Khanna, E. H. Linfield, A. G. Davies, H. Beere, and D. Ritchie, "Injection-locking of terahertz quantum cascade lasers up to 35GHz using RF amplitude modulation," Opt. Express **18**(20), 20799–20816 (2010).
22. D. Bachmann, M. Rösch, G. Scalari, M. Beck, J. Faist, K. Unterrainer, and J. Darmo, "Dispersion in a broadband terahertz quantum cascade laser," Appl. Phys. Lett. **109**(22), 221107 (2016).
23. L. Consolino, M. Nafa, F. Cappelli, K. Garrasi, F. P. Mezzapesa, L. Li, A. G. Davies, E. H. Linfield, M. S. Vitiello, P. De Natale, and S. Bartalini, "Fully phase-stabilized quantum cascade laser frequency comb," arXiv 1902.01604 (2019).

129.199.116.43 {ts '2024-10-15 04:06:32'}